On the Data Freshness for Industrial Internet of Things with Mobile Edge Computing

Jiaping Li, Jianhua Tang, *Member, IEEE*, and Zilong Liu, *Senior Member, IEEE*

***Abstract*—The paper studies the freshness of information with the aid of *age of information (AoI)* in the Industrial Internet of Things (IIoT) which plays a vital role to ensure quality and timely delivery of data services. To reduce the AoI, we leverage mobile edge computing (MEC) to partially offload information to the mobile edge server. Aiming to cope with the packet error in the setting of short packet communication (SPC) in IIoT, we consider the standard automatic repeat request (ARQ) protocol with two policies, i.e., either retransmitting an out-of-date packet (RO) or transmitting a freshest packet (TF), when a packet error occurs. We derive the closed-form of average AoI under these two policies respectively, and then formulate the average AoI minimization problem by jointly optimizing the short packet blocklength and MEC offloading ratio. Due to the nonconvexity nature of the problem, we tackle it by employing block coordinate descent (BCD) and successive convex approximation (SCA) methods and then prove their convergence. Our extensive numerical results show that the optimal average AoI yielded by our proposed approach is almost identical to that from the high-complexity exhaustive search method, and has significant improvement over the benchmark methods. From the AoI perspective, it is revealed that the optimal strategy tends to offload all information to mobile edge server when the computing capacity of local device is less than a threshold. Furthermore, it is found that the RO policy is suitable for the relatively small bandwidth and large local computing capability scenario, whilst the TF policy is better for the large bandwidth and small local computing capability case.**

***Index Terms*—Age of Information, Mobile Edge Computing, Short Packet Communication, Block Coordinate Descent, Successive Convex Approximation.**

I. Introduction

In recent years, the Industrial Internet of Things (IIoT) rapidly emerges as an instrumental component for the "Industrial 4.0". In IIoT, massive number of communication devices (e.g., machines, tablets, and sensors) are densely deployed over certain area for continuous environmental monitoring, surveillance, and data exchanges/analysis [2], [3]. Based on the real-time urgency levels of the collected data from various scenarios, different actions may take place. For example, super-rapid intervention is needed in a disastrous event (such as fire, earthquake, and flood), thus requiring ultra-reliable and low-latency communication (one of the major use cases in 5G-and-beyond networks).

Numerous research attempts have been made on IIoT. For instance, whilst [4] considers energy-effective resource allocation policy in a wireless power transfer system, [5] introduces the related security and privacy challenges as well as potential solutions in IIoT systems. However, besides the aspects above, one of the utmost requirements in IIOT is the data freshness. For instance, fresh temperature and humidity updates from sensors can help better predict and prevent industrial accidents in contrast to those obsolete updates which should be avoided in mission critical communications. Also, fresh knowledge of robots (e.g., moving direction, speed, and balance status) can better assist central monitoring system for necessary decisions/actions in a timely and accurate manner. Actually, in IIoT, fresh status data or information are widely required to ensure the accuracy of detection, prediction and decision making. In order to characterize the status updating and its impact to the system performance, a new metric, called age-of-information (AoI), has been proposed. Specifically, AoI, concerning the timeliness/freshness of certain data, is defined as the time elapsed since the latest correct delivery of the status update (that arrived at its intended destination) has been generated at its source [6].

Unlike the traditional quality of services (QoS) metrics such as communication latency, which represents the time that an information packet travels from the source to the destination, AoI reflects the freshness of the delivered status information from the destination's perspective. An AoI of certain status update at the destination can be divided into two parts:

- The first part is the time interval between when the source generates the information and when the destination correctly extracts the information from this packet. This part may be regarded as the communication delay of up-of-date successfully delivered packet, and hence AoI can be decreased by reducing the communication delay.
- The second part refers to the time interval from when the destination extracts the message to the current time before a new update information is received. The second part changes over time and AoI can be possibly cut down to the value of communication delay of a new update (at the time when it is correctly received by the destination). Thus, AoI can be reduced by reasonably speeding up the updating frequency.

J. Li and J. Tang are with Shien-Ming Wu School of Intelligent Engineering, South China University of Technology, China, e-mails: wijiapingli@mail.scut.edu.cn and jtang4@e.ntu.edu.sg. Z. Liu is with School of Computer Science and Electronics Engineering, University of Essex, UK, e-mail: zilong.liu@essex.ac.uk. The corresponding author is Jianhua Tang.

The work of J. Li and J. Tang was supported in part by the National Nature Science Foundation of China under Grant 62001168 and in part by the Foundation and Application Research Grant of Guangzhou under Grant 202102020515. The work of Z. Liu was supported in part by the UK Engineering and Physical Sciences Research Council under Grant EP/P03456X/1. Part of this paper [1] has been presented at the 10th International Workshop on Signal Design and its Applications in Communications (IWSDA'22), Colchester, United Kingdom, August 2022.

Since AoI is a more comprehensive concept than traditional QoS metrics, the existing techniques for minimizing communication delay or maximizing throughput may not be directly applied. Against this background, this paper aims to minimize the AoI with the aid of mobile edge computing (MEC).

A. Related Works

In [6], the authors derived the general expression of AoI with the information packets forwarded based on first-come-first-served (FCFS) principle, and obtained the optimal utilization factors of M/M/1, M/D/1, D/M/1 queuing models, respectively. Since the status update carries the Markov state of the source, the transmission of the youngest state packet can eliminate the need for transmission of the older packets in the queue. Therefore, the lossy last-come-first-served (LCFS) queuing discipline is reasonable for decreasing the age at the destination [7], [8]. The above papers concentrate on the model that the update packets are stochastically generated at the source. Another model is called generate-at-will model [9], [10], in which the status updates of certain process of interest can be sampled and generated at any time by the source node. Such a model is adopted in our work.

Moreover, there have been studies aiming for reducing AoI from its aforementioned two parts respectively. [6], [10] and [11] adopt the so-called zero-wait policy, also known as work-conserving policy in queuing theory, i.e., the source submits a fresh update once the transmitter or destination is free. In [12], the authors have shown that the zero-wait policy can achieve the minimum average delay and pointed out there exist better policies (e.g., waiting a moment) towards minimum AoI. Besides, non-orthogonal multiple access is also a promising technology to reduce the system AoI when multiple sources communicate over certain resource nodes [13]. In [14], the problem of reducing AoI has been studied with bandwidth and power constraints in multi-state time-varying channels. A comprehensive survey on AoI can be found in [15].

The above references only take into account the influence of queueing and data transmission delay with no consideration of the effect of data processing on AoI. In IIoT, the status data, which are generated via continuous environmental monitoring or detecting, may be large-sized and computation-intensive [3]. As a result, it could take a relatively long time to process the data due to the limited computational capacity of a local processor. In recent years, MEC has attracted tremendous research attention owing to its potential for significantly reducing the long processing time by offloading the data to a mobile edge server with adequate computational capacity. Motivated by this, in this work, we leverage the MEC technique and adopt the partial offloading model whose applications are composed of multiple fine-grained processes/components, such as augmented reality and fault detection. [11], [16] and [17] studied the AoI minimization problem in MEC or fog computing assisted network.

Considering that wireless channel may be unreliable and packet transmission may suffer from failure, standard automatic repeat request (ARQ) and hybrid ARQ are considered to minimize AoI [10], [18]. Furthermore, it is noted that sporadic short packet communication (SPC) is the dominant traffic in IIoT [19], in which finite blocklength codes are adopted due to the stringent latency requirement and normally a small amount of information (e.g., environment data) to be transmitted in IIoT [20]–[23]. In SPC, the communication capacity is also dependent on the blocklength of short packet [24]. The effect of packet blocklength on AoI has been investigated in [18] by leveraging the results of [24].

B. Our Contributions

In this work, we minimize the AoI by advocating the use of MEC to lower the data processing time. In particular, under SPC, we consider the standard ARQ protocol with two policies, i.e., either retransmitting an out-of-date packet (RO) or transmitting a freshest packet (TF), once a decoding failure occurs.[1] The main contributions of this paper are summarized as follows:

- We reduce the average AoI by partially offloading the data to mobile edge server and derive a closed-form average AoI as a function of the packet blocklength and the ratio of the local processing data, respectively.
- Due to the non-convexity of the average AoI, we take advantage of the block coordinate descent (BCD) and successive convex approximation (SCA) methods to obtain the optimal blocklength and offloading ratio. Besides, the convergence of the proposed approach is also proved.
- Numerical results show that our algorithm leads to rapid convergence rate, while the resultant optimal average AoI is almost identical as that by the exhaustive search method. An intriguing finding is that, regardless of the RO or TF policy, the optimal strategy inclines to offload all information bits to mobile edge server when the computing capacity/frequency of local device is less than certain threshold. Moreover, by comparing the average AoIs under these two policies and unlike the existing research results, we show that transmitting a freshest packet is not always better than retransmitting an older packet. In addition, whilst we observe that the RO policy is suitable for the relatively small bandwidth and large local computing capability scenario, whilst the TF policy is preferred in the case of large bandwidth and small local computing capability.

The rest of this paper is organized as follows. The system model and problem formulation are introduced in section II. In section III and IV, we analyse and solve the optimal average AoI under ARQ protocol and traditional protocol, respectively. In section V, we design an algorithm and prove its convergence. In section VI, the analysis of AoI and performance of algorithm are validated, and the RO policy and TF policy are compared through numerical results. Finally, section VII draws the conclusions.

II. System Model and Problem Formulation

We consider a status monitoring and control network as depicted in Fig. 1, where a sensor samples and generates

[1] Our previous work [1] is based on TF policy only. In this work, we analyze both RO and TF policies respectively and provide more insights with different system configurations.

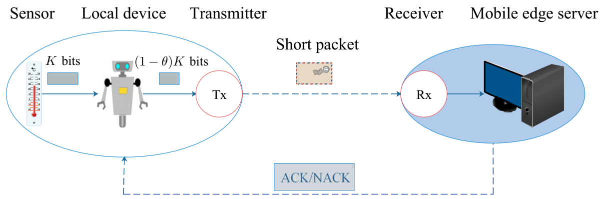

Fig. 1. System model

status update information first, then send it to the receiver by transmitter via wireless channel. Before each transmission, a portion of information is processed at the local device. Subsequently, the produced result (from local processing), together with the remaining part of the information are encoded into short packets and then forwarded to mobile edge server for further processing. Besides, the size of the produced result at the local device is neglected since it is normally very small.

In this system, if the destination (i.e., mobile edge server) fails to decode a packet, it will send out an NACK feedback to the source. Otherwise, an ACK feedback will be sent back. Regardless of whether RO policy or TF policy, once the source receives an ACK feedback, it would generate and forward a freshest status update. However, if the source receives an NACK feedback, in RO policy, it would retransmit the failed outdated packet. On the other hand, in TF policy, it would generate and forward a new status update instead. Moreover, to simplify our model, zero-wait policy is chosen, i.e., the source submits a/an fresh/old update once the destination is free.

Remark 1: In this work, we consider the zero-wait model where the source generates a new status packet only when the system is free. Therefore, there is no queueing delay during the transmission of status update. On the other hand, if there are multiple status packets in the network at the same time, they would queue and wait to be processed by local processor (and then forwarded to destination). Many existing works on AoI in queue-theoretic systems can be found in [6], [8] and [25].

A. AoI Model

The evolution of AoI under RO policy is illustrated in Fig. 2(a). Without loss of generality, we assume that the system starts at $t = 0$ and the age is $\Delta(0) = \Delta_0$. The AoI increases over time and drops down sharply once the destination receives the freshest status update. Since packet error exists in SPC, the system may utilize up to n_i transmission attempts for the i-th update, meaning that the first $n_i - 1$ transmitted packets are failed to be decoded until the n_i-th packet.

Let g_i denote the generation time of the i-th update. At time $c_{i,L}$, a part of information bits has been computed by the local device and the output is forwarded to wireless channel. A copy of the output is also stored in the local device until mobile edge server decodes update packet correctly. At time $d_i^{(j)}$, the destination receives and checks the packet for the j-th time, $j \in \{1, 2, ..., n_i\}$. If the packet is corrupted, the source will retransmit the (locally processed) old packet such as $d_{i+1}^{(1)}$

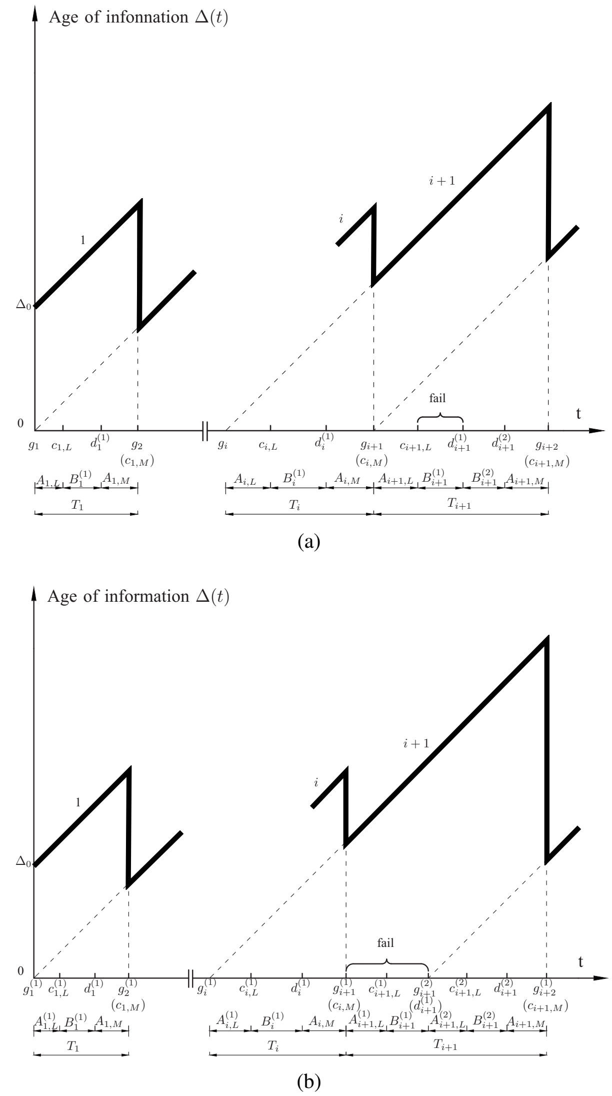

Fig. 2. The evolution of AoI. (a) RO policy. (b) TF policy.

in Fig. 2(a). At time $c_{i,M}$, the mobile edge server extracts the information of the i-th update correctly and finishes the i-th update, at the same time the sensor generates a new sample for the $(i+1)$-th update.

To characterize the process of update, we divide the time interval T_i for the i-th update into three type of time-slots. The local computing time-slot and mobile edge computing time-slot for the i-th update are denoted as $A_{i,L}$ and $A_{i,M}$, respectively. For the i-th update, the transmission time-slot of its j-th attempt is denoted as $B_i^{(j)}$. Thus, the update interval can be expressed as $T_i = g_{i+1} - g_i = A_{i,L} + \sum_{j=1}^{n_i} B_i^{(j)} + A_{i,M}$. We explain the characteristics of AoI based on RO policy as follows:

- We assume that the initial AoI Δ_0 is equal to T_0 and the sensor generates the first status sample at $t = 0$, i.e., $g_1 = 0$.
- The AoI increases linearly from $t = g_i$ to $t = g_{i+1}$.
- The value of AoI drops down to T_i at $t = g_{i+1}$.

The evolution of AoI based on TF policy is illustrated in Fig. 2(b). Different from RO policy, once an update is corrupted, a freshest sample is generated by sensor and then processed by local device before being transmitted to wireless channel. Therefore, an update under TF policy requires n_i local processing rounds. By contrast, it takes only one round in RO policy. Let $g_i^{(j)}$ denote the generation time of the j-th status sample for the i-th update. At time $c_{i,L}^{(j)}$, a part of the j-th sample information bits has been processed by the local device. Besides, denote by $A_{i,L}^{(j)}$ the local computing time-slot of the j-th attempt for the i-th update, and the update interval can be formulated as $T_i = g_{i+1}^{(1)} - g_i^{(1)} = \sum_{j=1}^{n_i}(A_{i,L}^{(j)} + B_i^{(j)}) + A_{i,M}$. We explain the characteristics of AoI based on TF policy as follows:

- We assume that the initial AoI Δ_0 is equal to T_0 and the sensor generates the first packet at $t = 0$, i.e., $g_1^{(1)} = 0$.
- The AoI increases linearly from $t = g_i^{(1)}$ to $t = g_{i+1}^{(1)}$.
- The value of AoI drops down to S_i at $t = g_{i+1}^{(1)}$, where $S_i = A_{i,L}^{(n_i)} + B_i^{(n_i)} + A_{i,M}$.

B. MEC Model

Considering the dependency and bit-wise correlation of data [26] [27], it is unpractical to partition the information into two independent parts and process them parallelly at the local device and the mobile edge server respectively [11]. In this paper, we consider the partial computing in tandem, where the local device firstly computes a part of information bits generated by sensor and the output, together with the remaining information bits, are transmitted to the mobile edge server for further processing. We denote the local processing ratio as θ, $\theta \in [0, 1]$. Moreover, the following analysis is based on the assumption that the size of sample information is identical at each update, namely K bits message, as depicted in Fig. 1. Thus, we omit the superscript (j) and subscript i of $A_{i,L}$, $A_{i,L}^{(j)}$ and $A_{i,M}$ hereafter. Hence for each update, there are θK bits processed at the local device and $(1-\theta)K$ bits are transmitted to the mobile edge server (we omit the output size of local processing).

We adopt a linear computation partitioning model [11], the computing time at the local device and the mobile edge server are expressed as

$$A_L = A_{i,L} = A_{i,L}^{(j)} = \frac{\theta CK}{f_L}, \ \forall i, \ j, \tag{1a}$$

$$A_M = A_{i,M} = \frac{(1-\theta)CK}{f_M}, \ \forall i, \tag{1b}$$

where C is the number of central process unit (CPU) cycles to process one bit information. The computing frequency (i.e., the CPU processing speed) of the local device and the mobile edge server are denoted as f_L and f_M, respectively.

C. Short Packet Model

We consider a delay-constrained communication system where the duration of packet transmission is smaller than the coherence time of channel. That is, the channel is quasi-static in that it remains constant over each packet transmission duration and varies independently among different packet transmission durations [19], [28]. Considering the small-scale fading and large-scale loss, the wireless channel is modeled as the Rayleigh fading model and the channel gain from the transmitter to the receiver is set as $h = d^{-\alpha}\mathcal{X}_0\tilde{h}$, where d represents the distance between transmitter and receiver, α denotes the path-loss exponent, $\mathcal{X}_0$ is the channel power gain at the reference distance, $\tilde{h}$ is an exponentially distributed random variable with unit mean that represents the short-term fading. Moreover, due to the short-term fading, we assume that only statistic channel state information (CSI) is available at the source.

According to [24], for a quasi-static Rayleigh channel, the maximum coding rate R at finite packet blocklength is given by

$$R \approx \ln(1+\gamma) - \sqrt{\frac{V}{m}}Q^{-1}(\varepsilon). \tag{2}$$

In (2), γ refers to the signal-to-noise ratio (SNR), i.e., $\gamma = \frac{hP}{N_0}$, where P denotes the transmission power of transmitter and N_0 represents the noise power seen at the receiver. V is the channel dispersion and given by $V = 1 - \frac{1}{(1+\gamma)^2}$, ε is packet decoding error rate, m is packet blocklength and $Q^{-1}(x)$ is the inverse function of $Q(x) = \int_x^\infty \frac{1}{2\pi}e^{-\frac{t^2}{2}}dt$.

After local computing, $(1-\theta)K$ bits are encoded into a short packet whose blocklength is m channel uses. Therefore, the coding rate R can be expressed as $\frac{(1-\theta)K\ln 2}{m}$ npcu (nat per channel use). Equation (2) can be rewritten as

$$\varepsilon \approx Q\left(\frac{\sqrt{m}\left(\ln(1+\gamma) - \frac{D}{m}\right)}{\sqrt{1-\frac{1}{(1+\gamma)^2}}}\right), \tag{3}$$

where $D = (1-\theta)K\ln 2$ nats. Since the channel varies among different packet duration, the transmission error rate of each packet is different and we denote the packet error rate of the j-th packet for the i-th update as $\varepsilon_i^{(j)}$. The random variables $\varepsilon_i^{(j)}$ are independent and identically distributed (i.i.d.), which are identically distributed with ε.

When $n_i = L$, meaning that the destination receives a correct packet for the first time after $L-1$ attempts of transmissions from the source, the distribution law of n_i is expressed as

$$P(n_i = L) = \varepsilon_i^{(1)}\varepsilon_i^{(2)}\cdots\varepsilon_i^{(L-1)}(1-\varepsilon_i^{(L)}) = \prod_{q=1}^{L-1}\varepsilon_i^{(q)}(1-\varepsilon_i^{(L)}). \tag{4}$$

Lemma 1: The expectation of n_i and n_i^2 are given by equations (5) and (6), where $\mathbb{E}(\varepsilon)$ denotes the expectation of ε.

$$\mathbb{E}(n_i) = \frac{1}{1-\mathbb{E}(\varepsilon)}. \tag{5}$$

$$\mathbb{E}(n_i^2) = \frac{1+\mathbb{E}(\varepsilon)}{\left(1-\mathbb{E}(\varepsilon)\right)^2}. \tag{6}$$

Proof: Please refer to Appendix A. □

D. Long-term Average AoI

The duration of packet transmission corresponds to $B = B_i^{(j)} = m\sigma$ seconds, where σ is the symbol duration that is equal to $1/W$ with W as the channel bandwidth [19].

In RO policy, as depicted in Fig. 2(a), during the i-th update, the area of rectangular trapezoid surrounded by AoI curve and time axes is calculated as $\frac{1}{2}(2T_{i-1}+T_i)T_i$. Combining former discussions, we set the length of the observation interval as $\tau = g_{N+1}$. Then the long-term average AoI is derived as

$$\begin{aligned}
\overline{\Delta}_{RO} &= \lim_{\tau\to\infty} \frac{1}{\tau} \int_0^{\tau} \Delta(t)\ dt \\
&= \lim_{N\to\infty} \frac{1}{g_{N+1}} \int_0^{g_{N+1}} \Delta(t)\ dt \\
&= \lim_{N\to\infty} \frac{\sum_{i=1}^{N} \frac{(2T_{i-1}+T_i)T_i}{2}}{\sum_{i=1}^{N} T_i} \\
&= \lim_{N\to\infty} \frac{\frac{1}{N}\sum_{i=1}^{N} \frac{(2T_{i-1}+T_i)T_i}{2}}{\frac{1}{N}\sum_{i=1}^{N} T_i} \\
&\overset{(a)}{=} \frac{\mathbb{E}^2(T)+\frac{1}{2}\mathbb{E}(T^2)}{\mathbb{E}(T)} \\
&= \mathbb{E}(T) + \frac{\mathbb{E}(T^2)}{2\mathbb{E}(T)},
\end{aligned} \tag{7}$$

where (a) holds, since in RO policy, $T_i = A_L + n_i B + A_M$ and T_{i-1} are i.i.d.

In TF policy as illustrated in Fig. 2(b), the area of rectangular trapezoid is formulated as $\frac{1}{2}(2S+T_i)T_i$, where $S = A_L + B + A_M$. Set the length of the observation interval $\tau = g_{N+1}^{(1)}$, the long-term average AoI is written as

$$\begin{aligned}
\overline{\Delta}_{TF} &= \lim_{\tau\to\infty} \frac{1}{\tau} \int_0^{\tau} \Delta(t)\ dt \\
&= \lim_{N\to\infty} \frac{1}{g_{N+1}^{(1)}} \int_0^{g_{N+1}^{(1)}} \Delta(t)\ dt \\
&= \lim_{N\to\infty} \frac{\sum_{i=1}^{N} \frac{(2S+T_i)T_i}{2}}{\sum_{i=1}^{N} T_i} \\
&= \lim_{N\to\infty} \frac{\frac{1}{N}\sum_{i=1}^{N} \frac{(2S+T_i)T_i}{2}}{\frac{1}{N}\sum_{i=1}^{N} T_i} \\
&= \frac{S\mathbb{E}(T)+\frac{1}{2}\mathbb{E}(T^2)}{\mathbb{E}(T)} \\
&= S + \frac{\mathbb{E}(T^2)}{2\mathbb{E}(T)}.
\end{aligned} \tag{8}$$

III. AoI ANALYSIS FOR RO POLICY

In this section, we aim to minimize the long-term average AoI based on RO policy by jointly optimizing the offloading ratio and packet blocklength. Since $\mathbb{E}(n_i)$ and $\mathbb{E}(n_i^2)$ are unrelated to i, we omit the subscript of n_i hereafter, i.e., $\mathbb{E}(n_i) = \mathbb{E}(n)$ and $\mathbb{E}(n_i^2) = \mathbb{E}(n^2)$. $\mathbb{E}(T)$ and $\mathbb{E}(T^2)$ are expressed as

$$\begin{aligned}
\mathbb{E}(T) =&\mathbb{E}(A_L + nB + A_M) \\
=&\frac{\theta CK}{f_L} + \frac{m}{W\left(1-\mathbb{E}(\varepsilon)\right)} + \frac{(1-\theta)CK}{f_M},
\end{aligned} \tag{9}$$

$$\begin{aligned}
\mathbb{E}(T^2) =&\mathbb{E}(A_L + nB + A_M)^2 \\
=&(A_L + A_M)^2 + \mathbb{E}(n^2)B^2 + 2\mathbb{E}(n)(A_L + A_M)B \\
=&\left(A_L + A_M + \mathbb{E}(n)B\right)^2 + \left(\mathbb{E}(n^2) - \mathbb{E}^2(n)\right)B^2 \\
=&\mathbb{E}^2(T) + \frac{m^2\mathbb{E}(\varepsilon)}{W^2\left(1-\mathbb{E}(\varepsilon)\right)^2}.
\end{aligned} \tag{10}$$

The approximation of $\mathbb{E}(\varepsilon)$ is presented by (11), which is accurate especially when the coding rate R is not very large [18, eq.(23)], where $\delta = \exp(\frac{D}{m}) - 1$ and $\overline{\gamma}$ is the expectation of SNR γ, i.e., $\overline{\gamma} = \frac{\mathcal{X}_0 d^{-\alpha} P}{N_0}$, since $\mathbb{E}(h) = \mathcal{X}_0 d^{-\alpha}$.

$$\mathbb{E}(\varepsilon) \approx 1 - \exp(-\frac{\delta - \frac{\sqrt{\pi D}}{m}}{\overline{\gamma}}). \tag{11}$$

Replacing $\mathbb{E}(\varepsilon)$ in (9) and (10) with (11), then the average AoI minimization problem under RO policy can be represented by

$$\begin{aligned}
\mathbf{P1}:\ \min_{\{\theta,m\}}\ \overline{\Delta}_{RO} = &\frac{3}{2}\left(\frac{\theta CK}{f_L} + \frac{(1-\theta)CK}{f_M} + \frac{m\mu}{W}\right) \\
&+ \frac{m^2(\mu^2-\mu)}{2W^2\left(\frac{\theta CK}{f_L} + \frac{(1-\theta)CK}{f_M} + \frac{m\mu}{W}\right)},
\end{aligned} \tag{12a}$$

$$s.t.\ 0 \le \theta \le 1, \tag{12b}$$

$$m_1 \le m \le m_2, \tag{12c}$$

$$m \in \mathbb{N}, \tag{12d}$$

where m_1 and m_2 are the minimum and maximum values of packet blocklength respectively, and $\mathbb{N}$ is the set of natural numbers. Besides,

$$\mu = \mathbb{E}(n) = \frac{1}{1-\mathbb{E}(\varepsilon)} = \exp\left(\frac{\exp(\frac{D}{m}) - 1 - \frac{\sqrt{\pi D}}{m}}{\overline{\gamma}}\right),$$

which is a function of θ and m, standing for the expectation of transmission attempts for an update.

Problem $\mathbf{P1}$ is nonconvex since the objective function is nonconvex and the constraint (12d) is discrete, which is difficult to solve directly. We first relax the integer variable m into real numbers, i.e, $m \in \mathbb{R}$, and then leveraging the BCD method [29] (also known as the alternative optimization method) to solve the relaxed $\mathbf{P1}$[2].

A. Offloading Ratio Optimization

For any given blocklength m, the relaxed $\mathbf{P1}$ is still a nonconvex optimization problem. By introducing a new slack variable $\omega = \frac{m}{W}\mu$, the relaxed $\mathbf{P1}$ can be reformulated as [30]:

$$\min_{\{\theta,\omega\}}\ \frac{3}{2}(\theta\nu_1 + \nu_2 + \omega) + \frac{\omega^2 - \frac{m}{W}\omega}{2(\theta\nu_1 + \nu_2 + \omega)}, \tag{13a}$$

$$s.t.\ \frac{m}{W}\mu \le \omega, \tag{13b}$$

$$0 \le \theta \le 1, \tag{13c}$$

[2]We refer to problem $\mathbf{P1}$ with $m \in \mathbb{R}$ as the relaxed $\mathbf{P1}$.

where $\nu_1 = (\frac{1}{f_L} - \frac{1}{f_M})CK$ and $\nu_2 = \frac{CK}{f_M}$, and inequality (13b) holds because of Lemma 2.

Lemma 2: The inequality constraint (13b) is active at the optimum of relaxed $\mathbf{P1}$.

Proof: Please refer to Appendix B. □

Furthermore, problem (13) can be expressed as

$$\min_{\{\theta,\omega\}} \underbrace{\frac{3}{2}(\theta\nu_1+\nu_2+\omega) + \frac{(\omega-\frac{m}{2W})^2}{2(\theta\nu_1+\nu_2+\omega)}}_{h_1(\theta,\omega)} \underbrace{-\frac{m^2}{8W^2(\theta\nu_1+\nu_2+\omega)}}_{h_2(\theta,\omega)}, \tag{14a}$$

$$s.t. \quad \frac{m}{W}\mu - \omega \le 0, \tag{14b}$$

$$0 \le \theta \le 1, \tag{14c}$$

where $h_1(\theta,\omega)$ is convex since $\frac{(\omega-\frac{m}{2W})^2}{\theta\nu_1+\nu_2+\omega}$ is quadratic-over-linear composition with affine function [31], $h_2(\theta,\omega)$ is concave and μ is a convex function of θ as well.

Problem (14) is a DC programming problem, which can be represented as a difference of two convex functions [32]. To deal with non-convexity, the successive convex approximation (SCA) technique can be applied at each iteration. We know that concave function is globally upper-bounded by its first-order Taylor expansion [31] with given local point $(\theta^{(r)},\omega^{(r)})$ at the r-th iteration, the upper bounds of $\overline{\Delta}_{RO}$ can be represented as

$$\begin{aligned}\min_{\{\theta,\omega\}} \ \overline{\Delta}^{ub,\theta} &= h_1(\theta,\omega) + h_2(\theta^{(r)},\omega^{(r)}) \\ &\quad + \nabla h_2(\theta^{(r)},\omega^{(r)})^{\mathbf{T}} \begin{bmatrix}\theta-\theta^{(r)} \\ \omega-\omega^{(r)}\end{bmatrix}, \\ s.t. \ \ & (14b) - (14c),\end{aligned} \tag{15}$$

where $\nabla h_2(\theta^{(r)},\omega^{(r)})$ is the gradient of $h_2(\theta,\omega)$ at point $(\theta^{(r)},\omega^{(r)})$ which is given by

$$\nabla h_2(\theta^{(r)},\omega^{(r)}) = \frac{m^2}{8W^2(\theta^{(r)}\nu_1+\nu_2+\omega^{(r)})^2}\begin{bmatrix}\nu_1 \\ 1\end{bmatrix}. \tag{16}$$

Problem (15) is convex which can be efficiently solved by standard convex optimization solvers such as CVX [31].

B. Short Packet Blocklength Optimization

For any given offloading ratio θ, the relaxed $\mathbf{P1}$ is also nonconvex. Similar to the previous subsection, by introducing a new slack variable $\omega = \frac{m}{W}\mu$, the relaxed $\mathbf{P1}$ can be expressed as

$$\min_{\{m,\omega\}} \frac{3}{2}(\nu_3+\omega) + \frac{\omega^2-\frac{m}{W}\omega}{2(\nu_3+\omega)}, \tag{17a}$$

$$s.t. \quad \frac{m}{W}\mu \le \omega, \tag{17b}$$

$$m_1 \le m \le m_2, \ m \in \mathbb{R}, \tag{17c}$$

where $\nu_3 = (\frac{1}{f_L} - \frac{1}{f_M})\theta CK + \frac{CK}{f_M}$, and constraint (17b) holds similarly due to Lemma 2.

Similarly, we can write further problem (17) as

$$\min_{\{m,\omega\}} \underbrace{\frac{3}{2}(\nu_3+\omega) + \frac{(\omega-\frac{m}{2W})^2}{2(\nu_3+\omega)}}_{h_3(m,\omega)} \underbrace{-\frac{m^2}{8W^2(\nu_3+\omega)}}_{h_4(m,\omega)}, \tag{18a}$$

$$s.t. \quad \underbrace{\frac{e^{\frac{D}{m}}-1}{\overline{\gamma}} - \log(\omega)}_{h_5(m,\omega)} \underbrace{+\log(\frac{m}{W}) - \frac{\sqrt{\pi D}}{m\overline{\gamma}}}_{h_6(m,\omega)} \le 0, \tag{18b}$$

$$m_1 \le m \le m_2, \ m \in \mathbb{R}, \tag{18c}$$

where $h_3(m,\omega)$ is convex and $h_4(m,\omega)$ is concave since $\frac{(\omega-\frac{m}{2W})^2}{\nu_3+\omega}$ and $\frac{m^2}{\nu_3+\omega}$ are quadratic-over-linear composition with affine function [31]. Besides, $h_5(m,\omega)$ is convex and $h_6(m,\omega)$ is concave. Problem (18) is also a DC programming problem, SCA technique is applied at each iteration as well. With given local point $(m^{(r)},\omega^{(r)})$ at the r-th iteration, the upper bounds of $\overline{\Delta}_{RO}$ and constraint (18b) which are received by their first-order Taylor expansions [31] can be expressed as

$$\begin{aligned}\min_{\{m,\omega\}} \ \overline{\Delta}^{ub,m} &= h_3(m,\omega) + h_4(m^{(r)},\omega^{(r)}) \\ &\quad + \nabla h_4(m^{(r)},\omega^{(r)})^{\mathbf{T}} \begin{bmatrix}m-m^{(r)} \\ \omega-\omega^{(r)}\end{bmatrix}, \\ s.t. \ \ & h_5(m,\omega) + h_6(m^{(r)},\omega^{(r)}) \\ &\quad + \left(\frac{1}{m^{(r)}} + \frac{\sqrt{\pi D}}{(m^{(r)})^2\overline{\gamma}}\right)(m-m^{(r)}) \le 0, \\ & m_1 \le m \le m_2, \ m \in \mathbb{R},\end{aligned} \tag{19}$$

where $\nabla h_4(m^{(r)},\omega^{(r)})$ is the gradient of $h_4(m,\omega)$ at point $(m^r,\omega^{(r)})$ which is written as

$$\nabla h_4(m^{(r)},\omega^{(r)}) = -\frac{1}{8W^2}\begin{bmatrix}\frac{2m^{(r)}}{\nu_3+\omega^{(r)}} \\ -\frac{(m^{(r)})^2}{(\nu_3+\omega^{(r)})^2}\end{bmatrix}. \tag{20}$$

At this point, the relaxed $\mathbf{P1}$ is transformed to convex optimization problem (19) which also can be efficiently solved by toolboxes.

IV. AoI analysis for TF policy

In this section, we investigate further the long-term average AoI based on TF policy. First, $\mathbb{E}(T)$ and $\mathbb{E}(T^2)$ are formulated as

$$\begin{aligned}\mathbb{E}(T) =& \mathbb{E}\left(n(A_L+B)+A_M\right) \\ =& \left(\frac{\theta CK}{f_L} + \frac{m}{W}\right)\frac{1}{1-\mathbb{E}(\varepsilon)} + \frac{(1-\theta)CK}{f_M},\end{aligned} \tag{21}$$

$$\begin{aligned}\mathbb{E}(T^2) =& \mathbb{E}\left(n(A_L+B)+A_M\right)^2 \\ =& A_M^2 + (A_L+B)^2\mathbb{E}(n^2) + 2A_M(A_L+B)\mathbb{E}(n) \\ =& \left((A_L+B)\mathbb{E}(n)+A_M\right)^2 \\ &+ (A_L+B)^2\left(\mathbb{E}(n^2)-\mathbb{E}^2(n)\right) \\ =& \mathbb{E}^2(T) + \left(\frac{\theta CK}{f_L} + \frac{m}{W}\right)^2 \frac{\mathbb{E}(\varepsilon)}{(1-\mathbb{E}(\varepsilon))^2}.\end{aligned} \tag{22}$$

Substituting $\mathbb{E}(\varepsilon)$ in (11) into (21) and (22), thus the average AoI minimization problem can be formulated as

$$\mathbf{P2}: \min_{\{\theta,m\}} \overline{\Delta}_{TF} = \frac{1}{2}\left(\frac{\theta CK}{f_L}+\frac{m}{W}\right)\mu+\varphi_1\theta+\frac{m}{W}+\varphi_2 + \frac{\left(\frac{\theta CK}{f_L}+\frac{m}{W}\right)^2(\mu^2-\mu)}{2\left((\frac{\theta CK}{f_L}+\frac{m}{W})\mu+\frac{(1-\theta)CK}{f_M}\right)}, \tag{23}$$

$$s.t.\ 0\le\theta\le 1,\quad m_1\le m\le m_2,\quad m\in\mathbb{N},$$

where $\varphi_1=(\frac{1}{f_L}-\frac{3}{2f_M})CK$ and $\varphi_2=\frac{3CK}{2f_M}$. Since problem $\mathbf{P2}$ is nonconvex, the same approach to problem $\mathbf{P1}$ can also be adopted in this section. We first relax problem $\mathbf{P2}$ and refer to problem $\mathbf{P2}$ with $m\in\mathbb{R}$ as the relaxed $\mathbf{P2}$.

A. Offloading Ratio Optimization

For any given blocklength m, the relaxed $\mathbf{P2}$ is still a nonconvex optimization problem. By introducing a new slack variable $s=(\frac{\theta CK}{f_L}+\frac{m}{W})\mu$, relaxed $\mathbf{P2}$ can be reformulated as

$$\min_{\{\theta,s\}} \frac{1}{2}s+\varphi_1\theta+\varphi_2+\frac{m}{W}+\frac{s^2-s\left(\frac{\theta CK}{f_L}+\frac{m}{W}\right)}{2\left(s+\frac{(1-\theta)CK}{f_M}\right)}, \tag{24a}$$

$$s.t.\ \left(\frac{\theta CK}{f_L}+\frac{m}{W}\right)\mu\le s, \tag{24b}$$

$$0\le\theta\le 1, \tag{24c}$$

where inequality (24b) holds because of Lemma 3.

Lemma 3: The inequality constraint (24b) is active at the optimum of relaxed $\mathbf{P2}$.

Proof: Please refer to Appendix C. □

Equation (24) can be transformed into the difference between two convex functions as follows:

$$\min_{\{\theta,s\}} \underbrace{\frac{1}{2}s+\varphi_1\theta+\varphi_2+\frac{m}{W}+\frac{\left(s-\frac{\theta CK}{2f_L}-\frac{m}{2W}\right)^2}{2\left(s+\frac{(1-\theta)CK}{f_M}\right)}}_{f_1(\theta,s)} \underbrace{-\frac{\left(\frac{\theta CK}{f_L}+\frac{m}{W}\right)^2}{8\left(s+\frac{(1-\theta)CK}{f_M}\right)}}_{f_2(\theta,s)}, \tag{25a}$$

$$s.t.\ \underbrace{\frac{e^{\frac{D}{m}}-1-\frac{\sqrt{\pi D}}{m}}{\overline{\gamma}}-\log(s)}_{f_3(\theta,s)}+\underbrace{\log\left(\frac{\theta CK}{f_L}+\frac{m}{W}\right)}_{f_4(\theta,s)}\le 0, \tag{25b}$$

$$0\le\theta\le 1, \tag{25c}$$

where $f_1(\theta,s)$ and $f_3(\theta,s)$ are convex, $f_2(\theta,s)$ and $f_4(\theta,s)$ are concave since $\frac{(s-\frac{\theta CK}{2f_L}-\frac{m}{2W})^2}{s+\frac{(1-\theta)CK}{f_M}}$ and $\frac{(\frac{\theta CK}{f_L}+\frac{m}{W})^2}{s+\frac{(1-\theta)CK}{f_M}}$ are quadratic-over-linear composition with affine function [31].

Problem (25) is a DC programming problem as well, similar to the previous section, the SCA technique is applied to approximate the $\overline{\Delta}_{TF}$ and constraint at each iteration. With given local point $(\theta^{(r)},s^{(r)})$ at the r-th iteration, the upper bounds of $\overline{\Delta}_{TF}$ and constraint (25b) can be expressed as

$$\begin{aligned}\min_{\{\theta,s\}}\ \overline{\Delta}^{ub,\theta} &= f_1(\theta,s)+f_2(\theta^{(r)},s^{(r)}) + \nabla f_2(\theta^{(r)},s^{(r)})^{\mathbf{T}}\begin{bmatrix}\theta-\theta^{(r)}\\ s-s^{(r)}\end{bmatrix},\\ s.t.\ & f_3(\theta,s)+f_4(\theta^{(r)},s^{(r)})+\frac{1}{\theta^{(r)}+\frac{mf_L}{CKW}}(\theta-\theta^{(r)})\le 0,\\ & 0\le\theta\le 1,\end{aligned} \tag{26}$$

where $\nabla f_2(\theta^{(r)},s^{(r)})$ is the gradient of $f_2(\theta,s)$ at point $(\theta^{(r)},s^{(r)})$ which is given by

$$\nabla f_2(\theta^{(r)},s^{(r)}) = \begin{bmatrix} -\frac{(\frac{\theta^{(r)}CK}{f_L}+\frac{m}{W})\left(\frac{2CK}{f_L}(s^{(r)}+\frac{(1-\theta^{(r)})CK}{f_M})+(\frac{\theta^{(r)}CK}{f_L}+\frac{m}{W})\frac{CK}{f_M}\right)}{8(s^{(r)}+\frac{(1-\theta^{(r)})CK}{f_M})^2} \\ \frac{(\frac{\theta^{(r)}CK}{f_L}+\frac{m}{W})^2}{8(s^{(r)}+\frac{(1-\theta^{(r)})CK}{f_M})^2}\end{bmatrix}. \tag{27}$$

Ultimately, relaxed $\mathbf{P2}$ is transformed into convex problem (26) which can be solved efficiently by convex optimization solvers.

B. Short Packet Blocklength Optimization

For any given offloading ratio θ, the relaxed $\mathbf{P2}$ is nonconvex as well. Similar to the previous subsection, by introducing a new slack variable $s=(\frac{\theta CK}{f_L}+\frac{m}{W})\mu$, the relaxed $\mathbf{P2}$ is written as

$$\min_{\{m,s\}} \frac{1}{2}s+\frac{m}{W}+\varphi_1\theta+\varphi_2+\frac{s^2-s\left(\frac{\theta CK}{f_L}+\frac{m}{W}\right)}{2(s+\varphi_3)}, \tag{28a}$$

$$s.t.\ \left(\frac{\theta CK}{f_L}+\frac{m}{W}\right)\mu\le s, \tag{28b}$$

$$m_1\le m\le m_2,\ m\in\mathbb{R}, \tag{28c}$$

where $\varphi_3=\frac{(1-\theta)CK}{f_M}$, and constraint (28b) holds similarly as Lemma 3. Also, we are able to reformulate problem (28) as

$$\min_{\{m,s\}} \underbrace{\frac{1}{2}s+\frac{m}{W}+\varphi_1\theta+\varphi_2+\frac{\left(s-\frac{\theta CK}{2f_L}-\frac{m}{2W}\right)^2}{2(s+\varphi_3)}}_{f_5(m,s)} \underbrace{-\frac{\left(\frac{\theta CK}{f_L}+\frac{m}{W}\right)^2}{8(s+\varphi_3)}}_{f_6(m,s)}, \tag{29a}$$

$$s.t.\ \underbrace{\frac{e^{\frac{D}{m}}-1}{\overline{\gamma}}-\log(s)}_{f_7(m,s)}+\underbrace{\log\left(\frac{\theta CK}{f_L}+\frac{m}{W}\right)-\frac{\sqrt{\pi D}}{m\overline{\gamma}}}_{f_8(m,s)}\le 0, \tag{29b}$$

$$m_1\le m\le m_2,\ m\in\mathbb{R}, \tag{29c}$$

where $f_5(m,s)$ is convex and $f_6(m,s)$ is concave since $\frac{(s-\frac{\theta CK}{2f_L}-\frac{m}{2W})^2}{s+\varphi_3}$ and $\frac{(\frac{\theta CK}{f_L}+\frac{m}{W})^2}{s+\varphi_3}$ are quadratic-over-linear composition with affine function [31]. Besides, $f_7(m,s)$ is convex and $f_8(m,\overline{s})$ is concave. Problem (29) is a DC programming problem as well, the same technique to problem (25) also applies to this problem. Hence, at the r-th iteration with known local point $(m^{(r)},s^{(r)})$, we need to solve the following convex problem:

$$\begin{aligned}\min_{\{m,s\}}\ \overline{\Delta}^{ub,m} &= f_5(m,s)+f_6(m^{(r)},s^{(r)})\\ &\quad+\nabla f_6(m^{(r)},s^{(r)})^{\mathbf{T}}\begin{bmatrix}m-m^{(r)}\\ s-s^{(r)}\end{bmatrix},\\ s.t.\quad & f_7(m,s)+f_8(m^{(r)},s^{(r)})\\ &+\left(\frac{1}{\frac{\theta CKW}{f_L}+m^{(r)}}+\frac{\sqrt{\pi D}}{(m^{(r)})^2\overline{\gamma}}\right)(m-m^{(r)})\le 0,\\ & m_1\le m\le m_2,\ m\in\mathbb{R},\end{aligned} \tag{30}$$

where $\nabla f_6(m^{(r)},s^{(r)})$ is the gradient of $f_6(m,s)$ at point $(m^{(r)},s^{(r)})$ which is given by

$$\nabla f_6(m^{(r)},s^{(r)})=\begin{bmatrix}-\frac{\frac{\theta CK}{f_L}+\frac{m^{(r)}}{W}}{4W(s^{(r)}+\frac{(1-\theta)CK}{f_M})}\\ \frac{(\frac{\theta CK}{f_L}+\frac{m^{(r)}}{W})^2}{8(s^{(r)}+\frac{(1-\theta)CK}{f_M})^2}\end{bmatrix}. \tag{31}$$

Now, the problem (28) is converted into a series of convex optimization problems which also can be solved by toolboxes efficiently.

V. Algorithm and Convergence

The proposed BCD approach to solve the relaxed $\mathbf{P1}$ and relaxed $\mathbf{P2}$ is summarized in Algorithm 1.

Algorithm 1 Block Coordinate Descent Algorithm for solving relaxed $\mathbf{P1}$ or $\mathbf{P2}$.

1: Initialize $\theta^{(0)}$ and $m^{(0)}$, let $r=0$
2: **repeat**
3: Solving problem (15) or (26) for given $m^{(r)}$, and obtaining $\theta^{(r+1)}$.
4: Solving problem (19) or (30) for given $\theta^{(r+1)}$, and obtaining $m^{(r+1)}$.
5: Update $r=r+1$.
6: **until** The convergence achieves.
7: Output $(\theta^{(r)},m^{(r)})$ as $(\theta^*,\hat{m})$.

Theorem 1: Algorithm 1 is convergent.

Proof: For brevity, we omit the subscript of $\overline{\Delta}_{RO}$ and $\overline{\Delta}_{TF}$, and denote them as $\overline{\Delta}$. First, in Step 3 of Algorithm 1, for given $m^{(r)}$, one has

$$\begin{aligned}\overline{\Delta}(\theta^{(r)},m^{(r)}) &\overset{(b)}{=} \overline{\Delta}^{ub,\theta}(\theta^{(r)},m^{(r)})\\ &\overset{(c)}{\ge} \overline{\Delta}^{ub,\theta}(\theta^{(r+1)},m^{(r)})\\ &\overset{(d)}{\ge} \overline{\Delta}(\theta^{(r+1)},m^{(r)}),\end{aligned} \tag{32}$$

where (b) in (32) holds since $\overline{\Delta}(\theta,m^{(r)})$ is expanded to $\overline{\Delta}^{ub,\theta}(\theta,m^{(r)})$ at point $\theta^{(r)}$ by applying first-order Taylor expansion in (15) or (26), which means that they have same objective value at $\theta^{(r)}$; (c) holds since the optimal solution of $\overline{\Delta}^{ub,\theta}(\theta,m^{(r)})$ is $\theta^{(r+1)}$; (d) holds since $\overline{\Delta}^{ub,\theta}(\theta,m^{(r)})$ is the upper bound of $\overline{\Delta}(\theta,m^{(r)})$. Second, in Step 4 of Algorithm 1, for given $\theta^{(r+1)}$, we can know

$$\begin{aligned}\overline{\Delta}(\theta^{(r+1)},m^{(r)}) &= \overline{\Delta}^{ub,m}(\theta^{(r+1)},m^{(r)})\\ &\ge \overline{\Delta}^{ub,m}(\theta^{(r+1)},m^{(r+1)})\\ &\ge \overline{\Delta}(\theta^{(r+1)},m^{(r+1)}),\end{aligned} \tag{33}$$

where (33) holds similarly as (32). Based on (32) and (33), it follows that

$$\overline{\Delta}(\theta^{(r)},m^{(r)})\ge\overline{\Delta}(\theta^{(r+1)},m^{(r+1)}), \tag{34}$$

which reveals that the objective value of relaxed $\mathbf{P1}$ and $\mathbf{P2}$ are non-increasing after each iteration. Moreover, since $\overline{\Delta}$ is always larger than zero, the convergence of Algorithm 1 is hence proved. □

Finally, since Algorithm 1 only produces the blocklength $m\in\mathbb{R}$, to find out the optimal blocklength $m^*\in\mathbb{N}$ for problem $\mathbf{P1}$ and $\mathbf{P2}$, the following step should be performed after the convergence of Algorithm 1:

$$m^*=\underset{m\in\{\lfloor\hat{m}\rfloor,\lceil\hat{m}\rceil\}}{\arg\min}\ \overline{\Delta}^{ub,m}(\theta^*,m), \tag{35}$$

where $(\theta^*,\hat{m})$ is the output from Algorithm 1. In consequence, the optimal solution for problem $\mathbf{P1}$ or $\mathbf{P2}$ is (θ^*,m^*).

VI. Numerical analysis

In this section, we present the numerical results to validate the effectiveness of our proposed approach. As suggested in [11], [17], we assume path-loss exponent $\alpha=2$, channel power gain at reference distance $\mathcal{X}_0=10^{-3}$, channel bandwidth $W=180$ kHz, noise power $N_0=10^{-9}$ Watt, transmit power $P=0.02$ Watt, and the distance between the transmitter and the receiver $d=100$ m. We set the CPU cycles to process one bit information $C=10^4$ cycles/bit, the computing frequency of mobile edge server $f_M=9\times10^9$ cycles/s. The packet blocklength can vary in the range of $m_1=100$ to $m_2=1000$ channel uses. Besides, our BCD algorithm tried two different initial values, i.e., $\theta=0$ and $m=m_2$, and $\theta=1$ and $m=m_1$. And we choose the better one as our result of BCD approach.

We first show the convergence behaviour of the proposed Algorithm 1 under $K=400$ bits and $f_L=1\times10^8$ cycles/s. As illustrated in Fig. 3, the algorithm converges very fast, i.e, no more than 10 iterations.

To validate the performance of our proposed BCD based approach to find out (θ^*,m^*), we compare it with the following benchmark algorithms:

- Exhaustive Search (ES) method: the optimal integer packet blocklength is searched inside the interval $[m_1,m_2]$.
- None Offloading (NO) strategy: All K information bits are processed at the local device. In this strategy, we let

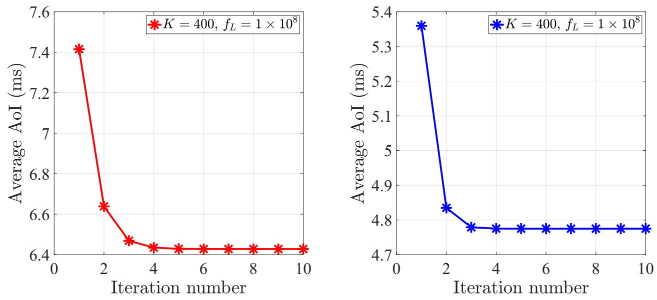

(a) (b)

Fig. 3. Convergence behaviour of the proposed Algorithm 1. (a) RO policy. (b) TF policy.

$m = m_1$ since no information bits (other than the output) need to be transmitted and the optimal blocklength here is just m_1.

- All Offloading (AO) strategy: All K information bits are offloaded to the mobile edge server. In this strategy, we let $m = m_2$ since the amount of information bits need to be transmitted is K, a much higher error rate and bigger AoI will be incurred if we choose a small m, i.e., $m = m_1$.
- Minimizing Delay (MD) method: Only the communication delay is considered and the corresponding offloading ratio and blocklength are obtained by minimizing the expectation of delay.

The change of average AoI under RO and TF policies by different amount of information are shown in Fig. 4. As illustrated, the minimum average AoI $\overline{\Delta}$ obtained by our proposed algorithm overlaps with that by the ES method, and it is smaller than those from the NO and AO strategies and MD method. Combining with the convergence rate as illustrated in Fig. 3, we verify the effectiveness of Algorithm 1. Furthermore, it can be observed that the average AoI increases with K grows, which verifies our intuition that the more information, the bigger AoI. In the mean time, we find that when the local device has sufficient computing capacity (e.g., $f_L = 1.5 \times 10^9$ cycles/s), the average AoI based on MD method is close to the optimal AoI (produced from ES). In addition, there is a cross between AO and NO strategies in Fig. 4(b). The reasons are: when K is small, the local server has the ability to process all information bits, thus NO is better than AO strategy; Nevertheless, as K increases, the local server with small computing frequency (e.g., $f_L = 1 \times 10^9$ cycles/s) cannot process all information bits in time and then AO becomes better than NO strategy. Besides, based on TF policy in Fig. 4(b), when $f_L = 1 \times 10^9$ cycles/s (low local computing frequency), the AoI of NO strategy is large than that of BCD approach; while at $f_L = 1.5 \times 10^9$ cycles/s (high local computing frequency), the AoI of NO strategy is close to that of BCD approach optimal. The reasons are:

- If the local device has adequate computing capacity, the optimal scheme is that local device processes as many information bits as possible and the optimal blocklength is $m = m_1$ which is similar to Fig. 5(b).
- Otherwise, less information bits are processed by local device and we need to find the optimal blocklength to encode all K information bits.

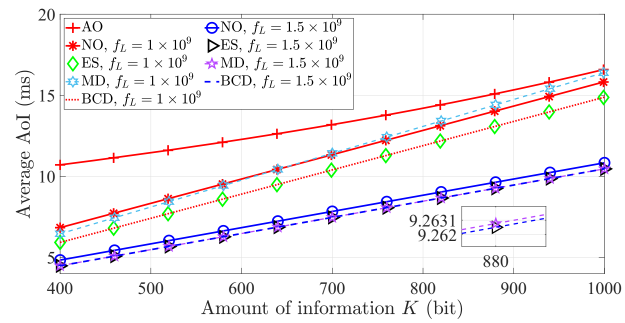

(a)

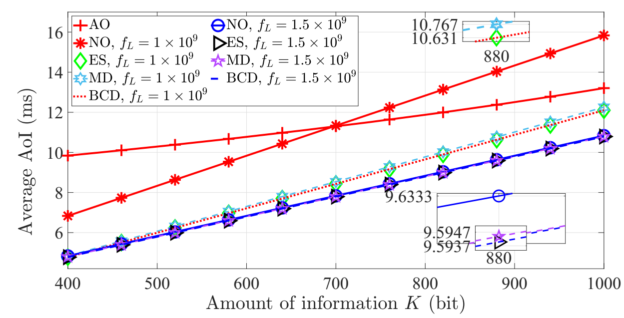

(b)

Fig. 4. Average AoI versus amount of information. (a) RO policy. (b) TF policy.

Fig. 5 describes the optimal blocklength and offloading ratio for different system configurations. We set $W = 180$ kHz and $f_L = 1 \times 10^8$ cycles/s in Fig. 5(a), $W = 20$ kHz and $f_L = 1 \times 10^9$ cycles/s in Fig. 5(b) and $W = 180$ kHz and $f_L = 1 \times 10^9$ cycles/s in Fig. 5(c), respectively. As illustrated in Fig. 5(a), whether RO or TF policy, the optimal offloading ratio is almost zero, namely the optimal strategy inclines to offload all information bits to the mobile edge server since the low local computing frequency and large channel bandwidth make it more suitable to process all the information bits at mobile edge server. Nevertheless, as depicted in Fig. 5(b), the optimal strategies under RO and TF policies both tend to process as many bits as possible at local device and the rest of information bits are encoded into short packet with minimal blocklength since it is more appropriate to process many bits at local device when the channel bandwidth is small and local device has enough computing capacity. Besides, in Fig. 5(c), we draw the optimal blocklength and offloading ratio under both high local computing frequency and large channel bandwidth.

Fig. 6 compares RO and TF policies when local device has a certain computing capacity. As illustrated in Fig. 6(a), it can be observed that when W is small, a slight increase of W gives rise to rapid decrease of AoI. Moreover, as illustrated in Fig. 6(b), when W is smaller than a certain threshold, $\overline{\Delta}_{RO}$ is less than $\overline{\Delta}_{TF}$, i.e., RO policy is better than TF policy from the AoI perspective.

Fig. 7 shows AoI comparison between RO and TF policies when local device has no computing capacity, i.e., local device does not process any data. As depicted in Fig. 7(b), TF policy

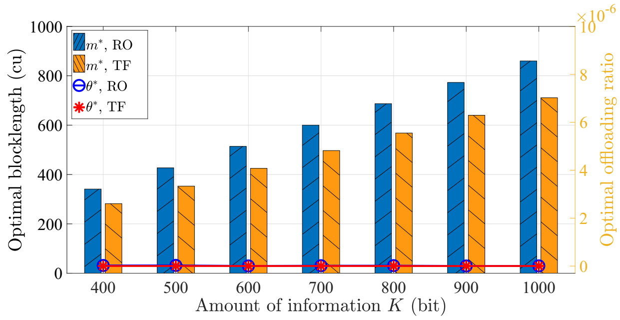

(a)

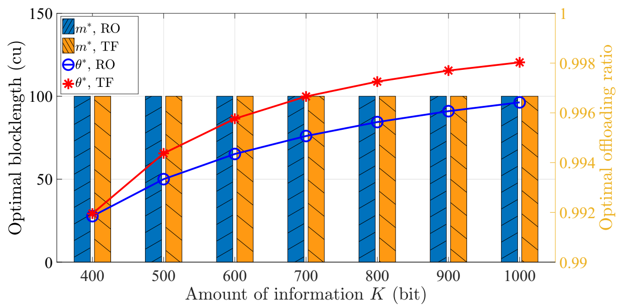

(b)

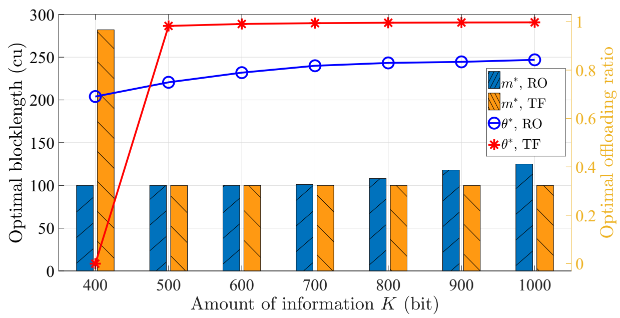

(c)

Fig. 5. Optimal blocklength and offloading ratio. (a) $W = 180$ kHz and $f_L = 1 \times 10^8$ cycles/s. (b) $W = 20$ kHz and $f_L = 1 \times 10^9$ cycles/s. (c) $W = 180$ kHz and $f_L = 1 \times 10^9$ cycles/s.

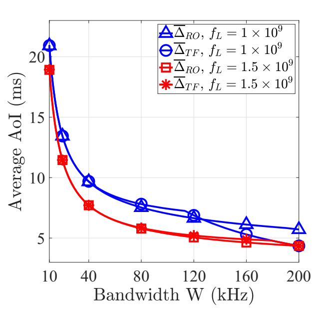

(a)

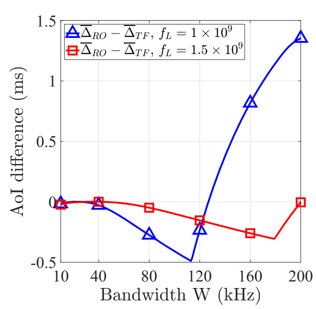

(b)

Fig. 6. (a) Average AoI and (b) difference value between AoI based on RO and TF policies versus bandwidth when $K = 400$ bits.

always outperforms RO policy when $f_L = 0$ cycles/s, meaning that there is no point in retransmitting a (failed) old status packet since the age of old status packet is larger than the age of freshest status packet [10].

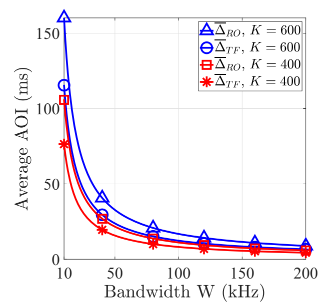

(a)

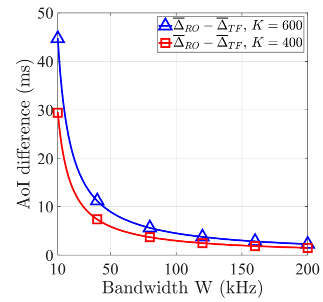

(b)

Fig. 7. (a) Average AoI and (b) difference value between AoI based on RO and TF policies versus bandwidth when $f_L = 0$ cycles/s.

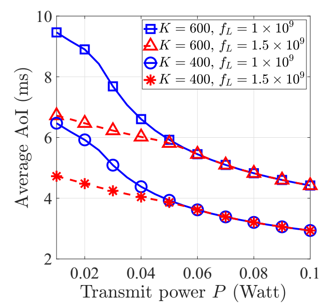

(a)

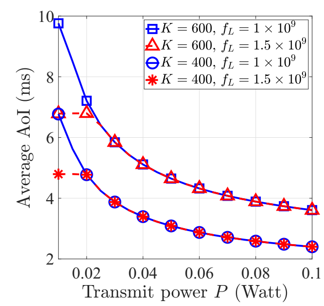

(b)

Fig. 8. Average AoI versus transmit power. (a) RO policy. (b) TF policy.

In Fig. 8, we evaluate how the transmit power P affects average AoI (produced by our proposed approach). As shown in Fig. 8, the average AoI decreases with growing P. Moreover, it can be observed that regardless of whether RO policy or TF policy, when P is less than a threshold, the average AoI generated from the one with high local computing frequency is smaller than that from low local computing frequency. However, when P is greater than the threshold, the two curves overlap as in this case, the optimal offloading strategy prefers offloading all K information bits to mobile edge server so that f_L has no influence on average AoI.

Fig. 9 depicts average AoI versus local computing frequency. It can be observed that, when f_L is small, the average AoI is not affected by f_L since if local device has no adequate computing capacity, the optimal offloading strategy tends to offload all information bits to mobile edge server as well. Moreover, when f_L is small, TF policy outperforms RO policy from the AoI perspective.

To conclude, if the system bandwidth is large and the local computing capacity is insufficient, TF policy is better, since the optimal offloading strategies under the two policies both incline to offload all information bits to mobile edge server and it makes no sense to retransmit a (failed) old packet when an update is failed; If the system bandwidth is small and the local computing capacity is sufficient, RO policy is better, since whether RO or TF policy, the optimal strategy inclines to process many information bits at the local device, and an update under TF policy requires multiple local processing rounds but RO policy requires only one round.

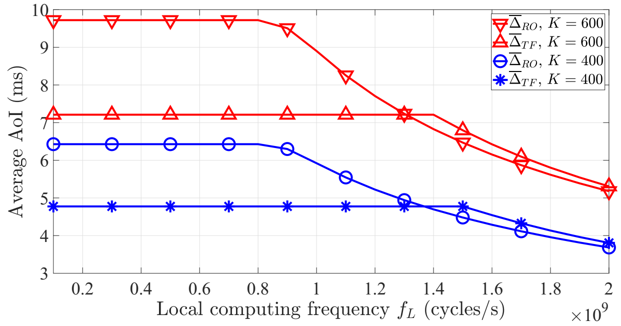

Fig. 9. Average AoI versus local computing frequency.

VII. Conclusions

In this paper, we have studied the problem of AoI minimization in MEC empowered IIoT where status packets may be wrongly decoded in the destination. Once a packet cannot be decoded correctly, the system retransmits an older update packet or a freshest update packet. We have devised the closed-form average AoIs under RO and TF policies respectively and minimized them by considering the blocklength and offloading ratio jointly. We have adopted the BCD and SCA techniques in order to tackle the formulated AoI minimization problem which is non-convex by nature. The numerical results show that our proposed algorithm enjoys stable convergence and outperforms the benchmark algorithms. Moreover, by comparing the typical RO and TF policies, we have identified the better policy for different system configurations through numerical results.

As a future work, we will extend this work to the multiple sensors scenario which is subject to certain resource constraints. Moreover, since AoI cannot reflect the content of a packet, an advanced information freshness metric is worthy of a closer investigation similar to [33], [34].

Appendix A
Proof of Lemma 1

The n_i is the compound random variable of $\varepsilon_i^{(j)}$, thus we can calculate the $\mathbb{E}(n_i)$ and $\mathbb{E}(n_i^2)$ as in equation (36) and equation (37), respectively.

$$\begin{aligned}
\mathbb{E}(n_i) =& \mathbb{E}_{\varepsilon_i^{(1)},\varepsilon_i^{(2)},\ldots,\varepsilon_i^{(\infty)}}\left(\mathbb{E}_{n_i}(n_i)\right)\\
=& \mathbb{E}_{\varepsilon_i^{(1)},\varepsilon_i^{(2)},\ldots,\varepsilon_i^{(\infty)}}\left(\sum_{l=1}^{\infty} lP(n_i=l)\right)\\
=& \mathbb{E}_{\varepsilon_i^{(1)},\varepsilon_i^{(2)},\ldots,\varepsilon_i^{(\infty)}}\left(\sum_{l=1}^{\infty} l(1-\varepsilon_i^{(l)})\prod_{q=1}^{l-1}\varepsilon_i^{(q)}\right)\\
=& \sum_{l=1}^{\infty}\mathbb{E}_{\varepsilon_i^{(1)},\varepsilon_i^{(2)},\ldots,\varepsilon_i^{(\infty)}}\left(l(1-\varepsilon_i^{(l)})\prod_{q=1}^{l-1}\varepsilon_i^{(q)}\right)\\
\overset{(e)}{=}& \sum_{l=1}^{\infty} l\left(1-\mathbb{E}(\varepsilon)\right)\mathbb{E}^{l-1}(\varepsilon)\\
=& \left(1-\mathbb{E}(\varepsilon)\right)\sum_{l=1}^{\infty}\left(\mathbb{E}^{l}(\varepsilon)\right)'\\
=& \frac{1}{1-\mathbb{E}(\varepsilon)}, \text{ and,}
\end{aligned} \tag{36}$$

$$\begin{aligned}
\mathbb{E}(n_i^2) =& \mathbb{E}_{\varepsilon_i^{(1)},\varepsilon_i^{(2)},\ldots,\varepsilon_i^{(\infty)}}\left(\mathbb{E}_{n_i}(n_i^2)\right)\\
=& \mathbb{E}_{\varepsilon_i^{(1)},\varepsilon_i^{(2)},\ldots,\varepsilon_i^{(\infty)}}\left(\sum_{l=1}^{\infty} l^2P(n_i=l)\right)\\
=& \mathbb{E}_{\varepsilon_i^{(1)},\varepsilon_i^{(2)},\ldots,\varepsilon_i^{(\infty)}}\left(\sum_{l=1}^{\infty} l^2(1-\varepsilon_i^{(l)})\prod_{q=1}^{l-1}\varepsilon_i^{(q)}\right)\\
=& \sum_{l=1}^{\infty}\mathbb{E}_{\varepsilon_i^{(1)},\varepsilon_i^{(2)},\ldots,\varepsilon_i^{(\infty)}}\left(l^2(1-\varepsilon_i^{(l)})\prod_{q=1}^{l-1}\varepsilon_i^{(q)}\right)\\
\overset{(f)}{=}& \sum_{l=1}^{\infty} l^2\left(1-\mathbb{E}(\varepsilon)\right)\mathbb{E}^{l-1}(\varepsilon)\\
=& \left(1-\mathbb{E}(\varepsilon)\right)\sum_{l=1}^{\infty}\left(\left(\mathbb{E}^{l+1}(\varepsilon)\right)''-\left(\mathbb{E}^{l}(\varepsilon)\right)'\right)\\
=& \frac{1+\mathbb{E}(\varepsilon)}{\left(1-\mathbb{E}(\varepsilon)\right)^2},
\end{aligned} \tag{37}$$

where (e) and (f) holds since the $\varepsilon_i^{(q)}$, $q \in \{1,2,\ldots\}$, are i.i.d. and identically distributed with ε.

Appendix B
Proof of Lemma 2

Equation (13a) can be rewritten as

$$\overline{\Delta}_{RO} = \underbrace{2\omega + \frac{(\theta\nu_1+\nu_2)(\frac{m}{W}+\theta\nu_1+\nu_2)}{2(\theta\nu_1+\nu_2+\omega)} + \theta\nu_1+\nu_2 - \frac{m}{2W}}_{G_1(\omega)},$$

where $G_1(\omega)$ is the function of ω. By taking the derivative of $G_1(\omega)$, it can be know that when $\omega \geq \omega_0$, $G_1(\omega)$ increases monotonically, where

$$\begin{aligned}
\omega_0 =& \frac{\sqrt{(\theta\nu_1+\nu_2)(\theta\nu_1+\nu_2+\frac{m}{W})}}{2} - (\theta\nu_1+\nu_2)\\
\overset{(g)}{\leq}& \frac{2(\theta\nu_1+\nu_2)+\frac{m}{W}}{4} - (\theta\nu_1+\nu_2) \leq \frac{m}{W}\mu,
\end{aligned}$$

where (g) holds because of the arithmetic-geometric mean inequality $\sqrt{ab} \leq \frac{a+b}{2}$. Thus, problem (13) obtains optimum when constraint (13b) reaches equality, otherwise we can always decrease ω without increasing the objective value $\overline{\Delta}_{RO}$.

Appendix C
Proof of Lemma 3

Equation (24a) can be reformulated as

$$\overline{\Delta}_{TF} = s + \frac{\left(\frac{CK(1-\theta)}{f_M}\right)^2 + \frac{CK(1-\theta)}{f_M}\left(\frac{CK\theta}{f_L} + \frac{m}{W}\right)}{2\left(s + \frac{CK(1-\theta)}{f_M}\right)} + \left(\frac{1}{2f_L} - \frac{1}{f_M}\right)CK\theta + \frac{m}{2W} + \frac{CK}{f_M}. \quad (38)$$

We regard $\overline{\Delta}_{TF}$ as the function of s and denote $\overline{\Delta}_{TF}$ as $G_2(s)$. By taking the derivative of $G_2(s)$, it can be obtained that when $s \geq s_0$, $G_2(s)$ increases monotonically, where

$$\begin{aligned} s_0 &= \frac{\sqrt{\frac{CK(1-\theta)}{f_M}\left(\frac{CK(1-\theta)}{f_M} + \frac{CK\theta}{f_L} + \frac{m}{W}\right)}}{\sqrt{2}} - \frac{CK(1-\theta)}{f_M} \\ &\overset{(h)}{\leq} \frac{\frac{2CK(1-\theta)}{f_M} + \frac{CK\theta}{f_L} + \frac{m}{W}}{2\sqrt{2}} - \frac{CK(1-\theta)}{f_M} \\ &\leq \left(\frac{CK\theta}{f_L} + \frac{m}{W}\right)\mu, \end{aligned}$$

where (h) holds due to the arithmetic-geometric mean inequality $\sqrt{ab} \leq \frac{a+b}{2}$. Therefore problem (24) attains optimal solution when constraint (24b) meets with equality, otherwise s can be cut down without increasing the objective value $\overline{\Delta}_{TF}$.

References

[1] J. Li, J. Tang, and Z. Liu, "Minimizing age of information for mobile edge computing empowered industrial Internet of things," in *Proc. 10th International Workshop on Signal Design and its Applications in Communications (IWSDA'22)*, Colchester, UK, Aug. 2022, pp. 1–5.

[2] L. D. Xu, W. He, and S. Li, "Internet of things in industries: A survey," *IEEE Trans. Ind. Informat.*, vol. 10, no. 4, pp. 2233–2243, Nov. 2014.

[3] E. Sisinni, A. Saifullah, S. Han, U. Jennehag, and M. Gidlund, "Industrial internet of things: Challenges, opportunities, and directions," *IEEE Trans. Ind. Informat.*, vol. 14, no. 11, pp. 4724–4734, Nov. 2018.

[4] L. Ji and S. Guo, "Energy-efficient cooperative resource allocation in wireless powered mobile edge computing," *IEEE Internet Things J.*, vol. 6, no. 3, pp. 4744–4754, Jun. 2019.

[5] A. Sadeghi, C. Wachsmann, and M. Waidner, "Security and privacy challenges in industrial internet of things," in *Proc. 52nd Annu. Des. Autom. Conf.*, San Francisco, CA, USA, Jun. 2015, pp. 1–6.

[6] S. K. Kaul, R. D. Yates, and M. Gruteser, "Real-time status: How often should one update?" in *Proc. IEEE INFOCOM*, Orlando, FL, USA, Mar. 2012, pp. 2731–2735.

[7] ——, "Status updates through queues," in *Conf. Inf. Sci. Syst. (CISS)*, Princeton, NJ, USA, Mar. 2012, pp. 1–6.

[8] R. D. Yates and S. K. Kaul, "The age of information: Real-time status updating by multiple sources," *IEEE Trans. Inf. Theory*, vol. 65, no. 3, pp. 1807–1827, Mar. 2019.

[9] I. Kadota, E. Uysal-Biyikoglu, R. Singh, and E. Modiano, "Minimizing the age of information in broadcast wireless networks," in *Proc. Annu. Allerton Conf. Commun. Control. Comput.*, Monticello, IL, USA, Sep. 2016, pp. 844–851.

[10] E. T. Ceran, D. Gündüz, and A. György, "Average age of information with hybrid ARQ under a resource constraint," in *Proc. IEEE Wireless Commun. Netw. Conf. (WCNC)*, Barcelona, Spain, Apr. 2018, pp. 1–6.

[11] Q. Kuang, J. Gong, X. Chen, and X. Ma, "Analysis on computation-intensive status update in mobile edge computing," *IEEE Trans. Veh. Technol.*, vol. 69, no. 4, pp. 4353–4366, Apr. 2020.

[12] Y. Sun, E. Uysal-Biyikoglu, R. Yates, C. E. Koksal, and N. B. Shroff, "Update or wait: How to keep your data fresh," in *Proc. IEEE INFOCOM*, San Francisco, CA, USA, Apr. 2016, pp. 1–9.

[13] A. Maatouk, M. Assaad, and A. Ephremides, "Minimizing the age of information: NOMA or OMA?" in *Proc. IEEE INFOCOM Workshop*, Paris, France, Apr. 2019, pp. 102–108.

[14] H. Tang, J. Wang, L. Song, and J. Song, "Minimizing age of information with power constraints: Multi-user opportunistic scheduling in multi-state time-varying channels," *IEEE J. Sel. Areas Commun.*, vol. 38, no. 5, pp. 854–868, May 2020.

[15] R. D. Yates, Y. Sun, D. R. Brown, S. K. Kaul, E. Modiano, and S. Ulukus, "Age of information: An introduction and survey," *IEEE J. Sel. Areas Commun.*, vol. 39, no. 5, pp. 1183–1210, May 2021.

[16] H. Zheng, K. Xiong, P. Fan, Z. Zhong, and K. B. Letaief, "Minimum age-energy aware cost in wireless powered fog computing networks," in *Proc. IEEE Int. Conf. Commun. (ICC)*, Dublin, Ireland, Jun. 2020, pp. 1–6.

[17] H. Wu, H. Tian, S. Fan, and J. Ren, "Data age aware scheduling for wireless powered mobile-edge computing in industrial internet of things," *IEEE Trans. Ind. Informat.*, vol. 17, no. 1, pp. 398–408, Jan. 2021.

[18] B. Yu, Y. Cai, D. Wu, and Z. Xiang, "Average age of information in short packet based machine type communication," *IEEE Trans. Veh. Technol.*, vol. 69, no. 9, pp. 10 306–10 319, Sep. 2020.

[19] G. Durisi, T. Koch, and P. Popovski, "Toward massive, ultrareliable, and low-latency wireless communication with short packets," *Proc. IEEE*, vol. 104, no. 9, pp. 1711–1726, Sep. 2016.

[20] J. Chen, L. Zhang, Y. Liang, X. Kang, and R. Zhang, "Resource allocation for wireless-powered IoT networks with short packet communication," *IEEE Trans. Wireless Commun.*, vol. 18, no. 2, pp. 1447–1461, Feb. 2019.

[21] B. Lee, S. Park, D. J. Love, H. Ji, and B. Shim, "Packet structure and receiver design for low latency wireless communications with ultra-short packets," *IEEE Trans. Commun.*, vol. 66, no. 2, pp. 796–807, Feb. 2018.

[22] C. She, C. Yang, and T. Q. S. Quek, "Radio resource management for ultra-reliable and low-latency communications," *IEEE Commun. Mag.*, vol. 55, no. 6, pp. 72–78, Jun. 2017.

[23] L. Zhang and Y. Liang, "Average throughput analysis and optimization in cooperative IoT networks with short packet communication," *IEEE Trans. Veh. Technol.*, vol. 67, no. 12, pp. 11 549–11 562, Dec. 2018.

[24] Y. Polyanskiy, H. V. Poor, and S. Verdu, "Channel coding rate in the finite blocklength regime," *IEEE Trans. Inf. Theory*, vol. 56, no. 5, pp. 2307–2359, May 2010.

[25] M. Moltafet, M. Leinonen, and M. Codreanu, "On the age of information in multi-source queueing models," *IEEE Trans. Commun.*, vol. 68, no. 8, pp. 5003–5017, 2020.

[26] Y. Mao, C. You, J. Zhang, K. Huang, and K. B. Letaief, "A survey on mobile edge computing: The communication perspective," *IEEE Commun. Surveys Tuts.*, vol. 19, no. 4, pp. 2322–2358, Fourthquarter 2017.

[27] P. Mach and Z. Becvar, "Mobile edge computing: A survey on architecture and computation offloading," *IEEE Commun. Surveys Tuts.*, vol. 19, no. 3, pp. 1628–1656, Thirdquarter 2017.

[28] W. Yang, G. Durisi, T. Koch, and Y. Polyanskiy, "Quasi-static multiple-antenna fading channels at finite blocklength," *IEEE Trans. Inf. Theory*, vol. 60, no. 7, pp. 4232–4265, Jul. 2014.

[29] J. C. Bezdek and R. J. Hathaway, "Some notes on alternating optimization," in *Advances in Soft Computing — AFSS 2002*. Berlin, Heidelberg: Springer Berlin Heidelberg, 2002, pp. 288–300.

[30] Q. Wu, Y. Zeng, and R. Zhang, "Joint trajectory and communication design for multi-UAV enabled wireless networks," *IEEE Trans. Wireless Commun.*, vol. 17, no. 3, pp. 2109–2121, Mar. 2018.

[31] S. Boyd and L. Vandenberghe, *Convex optimization*. Cambridge, U.K.: Cambridge University Press, 2004.

[32] Y. Sun, P. Babu, and D. P. Palomar, "Majorization-minimization algorithms in signal processing, communications, and machine learning," *IEEE Trans. Signal Process.*, vol. 65, no. 3, pp. 794–816, Feb. 2017.

[33] A. Maatouk, S. Kriouile, M. Assaad, and A. Ephremides, "The age of incorrect information: A new performance metric for status updates," *IEEE/ACM Trans. Netw.*, vol. 28, no. 5, pp. 2215–2228, Oct. 2020.

[34] W. Lin, X. Wang, C. Xu, X. Sun, and X. Chen, "Average age of changed information in the internet of things," in *Proc. IEEE Wireless Commun. Netw. Conf. (WCNC)*, Seoul, South Korea, May 2020, pp. 1–6.

Jiaping Li received the bachelor's degree from the School of Mechanical Engineering, Dongguan University of Technology, Dongguan, China, in 2018. He is currently pursuing the master's degree in Shien-Ming Wu School of Intelligent Engineering, South China University of Technology, China. His research interests include age of information and reinforcement learning.

Jianhua Tang (S'11-M'15) received the B.E. degree in communications engineering from Northeastern University, China, in 2010, and the Ph.D. degree in electrical and electronic engineering from Nanyang Technological University, Singapore, in 2015. He was a Post-Doctoral Research Fellow with the Singapore University of Technology and Design from 2015 to 2016, and a Research Assistant Professor with the Department of Electrical and Computer Engineering, Seoul National University, from 2016 to 2018. He is currently an Assistant Professor with the Shien-Ming Wu School of Intelligent Engineering, South China University of Technology. His research interests include edge computing, network slicing and industrial Internet of Things.

He was honored with the 2020 IEEE Communications Society Stephen O. Rice Prize. He is currently serving as an Editor for the IEEE WIRELESS COMMUNICATIONS LETTERS.

Zilong Liu is a Lecturer (Assistant Professor) at the School of Computer Science and Electronic Engineering, University of Essex. He received his PhD (2014) from School of Electrical and Electronic Engineering, Nanyang Technological University (NTU, Singapore), Master Degree (2007) in the Department of Electronic Engineering from Tsinghua University (China), and Bachelor Degree (2004) in the School of Electronics and Information Engineering from Huazhong University of Science and Technology (HUST, China). From Jan. 2018 to Nov. 2019, he was a Senior Research Fellow at the Institute for Communication Systems (ICS), Home of the 5G Innovation Centre (5GIC), University of Surrey. Prior to his career in UK, he spent nine and half years in NTU, first as a Research Associate (Jul. 2008 to Oct. 2014) and then a Research Fellow (Nov. 2014 to Dec. 2017). His research lies in the interplay of coding, signal processing, and communications.

He is an Editor of IEEE Wireless Communications Letters, IEEE Access, Frontiers in Communications and Networks, and Frontiers in Signal Processing. So far, he has published over 100 peer-reviewed journal/conference papers including more than 40 IEEE Transactions papers. Details of his research can be found at: https://sites.google.com/site/zilongliu2357.